

## Single-walled Boron Nitride Pores as Media for Hydrogen Storage: DFT and IGM Study

I.K. Petrushenko\*

*Irkutsk National Research Technical University, 83, Lermontov St., 664074 Irkutsk, Russia*

(Received 29 April 2019; revised manuscript received 02 August 2019; published online 22 August 2019)

The search of novel hydrogen storage media is of importance for the transfer to the 'green' hydrogen energetics. In this paper, we study hydrogen physisorption on single-walled boron nitride pores (BN) by means of DFT-D3 calculations. A variety of structures, ranging from the planar one to hollow pore models, was involved. It was founded that deep pore models adsorb H<sub>2</sub> molecules significantly stronger (adsorption energy, E<sub>a</sub>, of -11.41 to -19.77 kJ/mol) than planar h\_BN (-3.55 kJ/mol) and slightly bent 5\_BN (6.77 kJ/mol). Additional independent gradient model (IGM) analysis was employed to visualize interacting regions between hydrogen and a series of adsorbents. We also clearly reveal the atoms of adsorbents and the adsorbate molecule participating in the interaction more. We unambiguously show that peripheral atoms of the adsorbents give nearly negligible input in the total non-covalent interactions. The present results should expand our understanding of the fundamental basis of hydrogen storage using BN pore models.

**Keywords:** h\_BN, Boron nitride, Hydrogen, DFT, Adsorption, Pore.

DOI: [10.21272/jnep.11\(4\).04016](https://doi.org/10.21272/jnep.11(4).04016)

PACS numbers: 31.15.E- , 61.48.De,  
68.43. - h, 68.43.Bc.

### 1. INTRODUCTION

At present, there exists a tremendous scientific interest, which is devoted to hydrogen as an energy source [1]. There are some important issues, however, that slow down the ultimate transfer to hydrogen energetics, and they, therefore, are to be overcome: massive hydrogen production, its purification, storage, and delivery. Nowadays, the widely used approaches based on liquefying and pressurizing hydrogen exhibit numerous safety issues. Solid-state storage is thus being studied as a viable alternative. The significant attention of both theoreticians and experimentalists focuses on finding the novel solid-state storage systems for the effective hydrogen uptake [2].

Carbon as an earth-abundant element is widely used for hydrogen storage. Carbon nanotubes (CNTs) and graphene, allotropic forms of carbon, have been thoroughly studied from the H<sub>2</sub> storage point of view [3]. It was founded that physisorption on pristine graphene or outer walls of CNTs relies on weak van der Waals forces, which makes impossible their usage at room temperatures as adsorbents. Chemical H<sub>2</sub> storage is more promising for the high-temperature hydrogen capture; however, the hydrides suffer from poor reversibility. There is also a graphene counterpart, namely boron nitride (BN), which was introduced as a promising candidate for hydrogen storage in 2002 [4].

Following comprehensive works of Lian et al. [5] and Li et al. [6], one can select four factors for BN, which affect its high H<sub>2</sub> storage properties. Firstly, the large specific surface area of BN increases its sorption ability. Secondly, a large pore volume in BN increases the physical adsorption of H<sub>2</sub>. Thirdly, the ionic character of the B-N bond results in an enhanced electron transfer from chemisorbed H<sub>2</sub> to the electron-deficient B atom. Finally, there exist structural defects that offer strong bonding sites and enhanced dissociation of chemisorbing H<sub>2</sub>.

It can be easily seen that BN is a promising candidate for hydrogen storage, however, as widely known, hydrogen adsorption on planar surfaces is rather scarce [7]. Therefore, we should expand our knowledge on the hydrogen adsorption in the pores. Although several papers study such an adsorption in graphene pores, little information exists on the adsorption in the pores of BN. We found only a recent experimental work on BN porous microbelts, which have been successfully synthesized [8]. They provide reversible H<sub>2</sub> uptake at moderate conditions. Another paper is devoted to the adsorption of different organic compounds on porous BN samples [9].

In the present work, we explore the H<sub>2</sub> adsorption on bowl-shape pore models (for the purpose of comparison, we also use a planar structure as a representative of hexagonal BN (h\_BN) and then going to pore models of various depths). Herein, we address the following questions: firstly, because of the various depths of the involved adsorbent structures, the obtained results may shed light on the weak interactions between H<sub>2</sub> and other curved nanostructures. Secondly, considering the numerous available works on the synthesis of open fullerenes [10], and the comparatively large volumes inside the cavities of such fullerenes, it may be possible to store H<sub>2</sub> inside them. Finally, as it was mentioned above, the pore models may represent the cavities in bulky boron nitride, which has recently taken a marked role in the field of hydrogen storage. Besides this, it is worth studying evolution of the hydrogen adsorption energy (E<sub>a</sub>) on going from pores with small depths to the deepest ones. To this end, we employ the dispersion-corrected density functional theory method (DFT-D3). By using novel independent gradient model (IGM) approach, we visualize the atoms contributing to the interactions more. The obtained results are certain to be useful for further investigations on the non-covalent interactions between hydrogen molecules and boron nitride nanostructures.

---

\* [igor.petrushenko@istu.edu](mailto:igor.petrushenko@istu.edu)

## 2. COMPUTATIONAL METHODS

To make the models of deep hollow pores, we use the fullerene cluster ( $C_{70}$ ), in which we substitute carbon atoms with boron and nitrogen in an alternate manner. We then gradually delete 10, 20, 30 and 40 atoms *via* step-by-step removal, and obtain four bowl-shape hollow pores of different depths:  $B_{30}N_{30}H_{10}$  (1\_BN),  $B_{25}N_{25}H_{10}$  (2\_BN),  $B_{20}N_{20}H_{10}$  (3\_BN), and  $B_{15}N_{15}H_{10}$  (4\_BN) (Fig. 1). All the peripheral bonds were saturated with hydrogen atoms to avoid the dangling. Also, we use the corannulene-like molecule (5\_BN ( $B_{11}N_{19}H_{10}$ )) as the model with the smallest depth, and, finally, the coronene-like molecule ( $B_{12}N_{12}H_{10}$ ) was adopted as the model of planar hexagonal boron nitride (h\_BN). The depths of pores have been determined as follows: the length of the normal dropped from the plane of peripheral B and N atoms at the open end to the close end of the model.

Full geometry optimization of all structures has

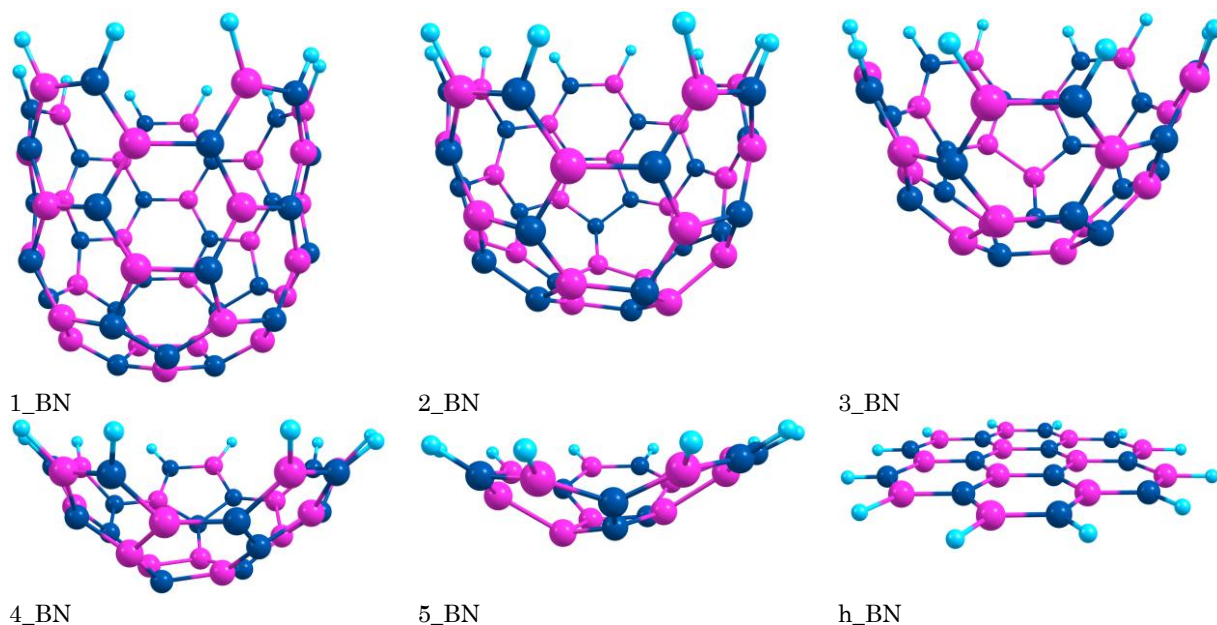


**Fig. 1** – The boron nitride (BN) hollow pore adsorbents involved in this work. Atomic color code: blue balls are nitrogen, magenta balls are boron, small light-blue balls are hydrogen

## 3. RESULTS AND DISCUSSION

### 3.1 Non-covalent Interactions between $H_2$ and BN Pore Models

First, we compare  $H_2$  adsorption onto the flat (h\_BN) and the slightly bent structure (5\_BN) (Fig. 1). As it was mentioned earlier [7, 14], the concave side of bent structures is more energetically favorable for hydrogen adsorption than the convex side as well as the adsorption on the planar structures. Indeed, calculated  $E_a$  of about  $-6.77$  and  $-3.55$  kJ/mol for 5\_BN and BN, respectively, i.e. there is a strong influence of the curved surface (Table 1). To validate the present results, we compare them with those obtained elsewhere.

Mpourmpakis et al. reported the following data for the (9.9) BN nanotubes (BNNTs):  $E_a$  of  $H_2$  interacting with the N atom is  $\sim -3.6$  kJ/mol and is  $\sim -2.6$  kJ/mol when  $H_2$  interacts with the B atom (B3LYP method)

been performed at the BLYP/def2-SVP level of theory, using the Orca 4.0.1 program [11]. The D3 correction for dispersion of Grimme et al. [12] was used in order to properly model the dispersion interactions. BLYP has been shown to be a very reliable density functional that suits well for the adsorption studies [13]. Adsorption energies have been calculated with the following equation:

$$E_a = E(\text{adsorbent}/H_2) - E(\text{adsorbent}) - E(H_2),$$

where  $E(\text{adsorbent} + H_2)$  is the energy of the studied complexes consisting of hollows and  $H_2$ ,  $E(\text{adsorbent})$  is the energy of the pore model, and  $E(H_2)$  is the energy of the hydrogen molecule, respectively. According to such a definition, a negative adsorption energy value means that bonding is energetically favorable. To eliminate the basis set superposition error (BSSE), we used the counterpoise correction of Boys and Bernardi.

[15]. The previous work of Petrushenko et al. yielded the following  $E_a$  values: from  $-3.5$  to  $-5.9$  kJ/mol (B3LYP-D3 method) [16]. The direct comparison is not possible as the different methods are used in the papers mentioned above. We can see that the results obtained herein are in a very good agreement with those already published.

We then turn to the adsorption on deeper pore models. Herein, we also consider adsorption on the inner sides of the hollow pore models. For deep pore models,  $E_a$  obtained can be compared to those determined for h\_BN and 5\_BN. In the case of 4\_BN, the hydrogen  $E_a$  was determined to be  $-11.41$  kJ/mol, i.e. considerably higher than those for h\_BN ( $-3.55$  kJ/mol) and for 5\_BN ( $-6.77$  kJ/mol). One may note here a clear trend: the more the dipole moment, the larger  $E_a$ . Indeed, for the last three models, their dipole moments are equal to 3.32 (4\_BN), 2.790 (5\_BN), and 0.144 (h\_BN) debye.

**Table 1** – Adsorption energies, bowl depths, and dipole moments for studied adsorbents

Adsorbent	$E_a$ , kJ/mol	Bowl depth, Å	Dipole moment, debye
1_BN	−19.77	6.605	4.618
2_BN	−18.73	5.282	4.434
3_BN	−15.80	4.009	4.150
4_BN	−11.41	2.557	3.932
5_BN	−6.77	1.254	2.790
h_BN	−3.55	0.000	0.144

The interaction of the permanent dipole (pore) – induced dipole (hydrogen) type increases polarization energy, and, thereby, adsorption energy. However, there exist large dispersion interactions, especially in the case of deep pores.

We further examine the following models: 1\_BN – 3\_BN. There are substantial  $E_a$  energy gaps between 4\_BN and 3\_BN (4.39 kJ/mol) and between 3\_BN and 2\_BN (2.93 kJ/mol) (Table 1). The further transition to the deepest 1\_BN model is accompanied by the comparatively small energy increment (1.03 kJ/mol). As a whole, the large increase in  $E_a$  on going from h\_BN (−3.55 kJ/mol) to 1\_BN (−19.77 kJ/mol) exists. In terms of energetic considerations, for a single  $H_2$  molecule, the values determined for the larger pores seem more suitable for hydrogen storage ( $\sim 20$  kJ/mol). It is worth comparing the results of the present work and the data on hydrogen storage obtained elsewhere.

Thus, for example, Sun et al. theoretically predicted that a fullerene  $C_{60}$  can be coated with twelve Li atoms on which total 60  $H_2$  molecules can be adsorbed with  $E_a$  of −7.23 kJ/mol per  $H_2$  [17]. Wu et al. suggested that Li-coated boron carbide nanotubes could store  $H_2$  with the binding energy in the range of −10 to −24 kJ/mol [18]. Gao et al. designed fullerene-based networks for hydrogen storage [19]. They computed  $E_a$  to be −27.96 kJ/mol. Zhou et al. have theoretically studied hydrogen storage on Li-doped defective graphene with boron substitution. They predicted the following values for  $E_a$ : from −19.28 to −38.56 kJ/mol [20]. Isidro-Ortega et al. have studied hydrogen storage on zeolite templated carbon (ZTC). They proved that the nanostructure ZTC system decorated with lithium atoms suits well for hydrogen storage with  $E_a$  of −12.05 to −12.73 kJ/mol [21]. Chen et al. studied hydrogen storage ability of carbon nanohorns. Li-decorated nanohorns provide high  $E_a$  of −15.42 to −31.81 kJ/mol [22]. Our previous paper on hollow carbon models presented the values from −20.13 to −20.86 kJ/mol [7]. An observation to be made is that the values of the adsorption energies obtained herein is similar to those for  $H_2$  on graphene and other related materials. A direct comparison with the theoretical works is not possible because the above mentioned authors used another DFT formalism in their works.

### 3.2 Independent Gradient Model (IGM) Analysis for BN Pore Models

The non-covalent interactions between the  $H_2$  molecule and the BN pores can be visualized by the Independent Gradient Model (IGM) method. It is based on the non-covalent interaction (NCI) index, which was recently developed by Yang et al. for the visualization

of noncovalent interactions [23]. More recently, Lefebvre et al. have developed IGM, a new electron density gradient ( $\nabla\rho$ ) based approach to identify and isolate the interactions between molecules or, more accurate, between user-defined fragments [24]. The new descriptors, which are defined in the framework of this method, allow obtaining a measure of electron sharing ( $\delta g = |\nabla\rho IGM| - |\nabla\rho|$ ), and separately describe interactions inside each molecule (fragment) ( $\delta g^{\text{intra}}$ ) or between molecules (fragments) ( $\delta g^{\text{inter}}$ ).

Fig. 2 shows the scatter graphs  $\delta g^{\text{inter}}/\delta g^{\text{intra}}$  vs.  $\text{sign}(\lambda_2)\rho$  for the two adsorbent models located on both ends of the studied series, namely, 1\_BN (the deepest pore) and h\_BN (the planar structure). Now we identify the character of the peaks on these graphs. The peaks corresponding to the interfragment interactions are colored in red, and those corresponding to the intrafragment ones are colored in black. The positive  $\text{sign}(\lambda_2)\rho$  values denote repulsion, and the negative ones denote attractive interactions. The obtained graphs are different for both structures. For the simpler case of h\_BN, we may have one peak, where  $\text{sign}(\lambda_2)\rho$  is 0.040. It corresponds to the weak steric region in 6-membered rings of h\_BN. We also observe two peaks in the range corresponding to the covalent interactions (B-N and H-B/N bonds). To assign the peaks, we made the IGM analysis on the h\_BN model without all H atoms. The obtained data clearly shows that large peak at *ca.* −0.200 corresponds to the B-N covalent bonds. The two small peaks at low  $\text{sign}(\lambda_2)\rho$  values imply that there is a weak non-covalent interaction

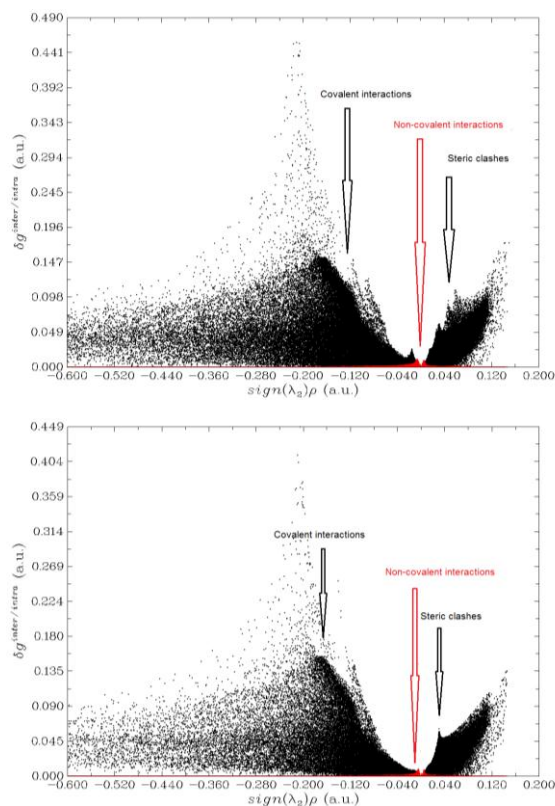


**Fig. 2** – The scatter graphs  $\delta g^{\text{inter}}/\delta g^{\text{intra}}$  vs.  $\text{sign}(\lambda_2)\rho$  for  $H_2/1\_BN$  (top) and  $H_2/h\_BN$  (bottom). The black and red areas correspond to intermolecular and intramolecular interactions, respectively

between h\_BN and a hydrogen molecule. The corresponding isosurfaces are presented in Fig. 3.

For 1\_BN, we observe numerous peaks in the ranges corresponding to both covalent interactions and steric clashes. It presumes that there exist various types of rings in the pore model. They are the following: a 6-membered ring like that observed in the case of h\_BN, a 5-membered ring, and a 6-membered ring including

B-B or N-N bonds (the positive range of 0.040-0.080). Analogously, for the covalent range, we can see the three peaks. The first of them is similar to that of the h\_BN case (at *ca.*  $-0.200$ ) and it corresponds to the B-N bonds. The second at *ca.*  $-0.120$  can be ascribed to the H-B/N bonds. The last peak at *ca.*  $-0.100$  corresponds to the B-B or N-N bonds. For this case, the interfragment non-covalent interactions also exist.

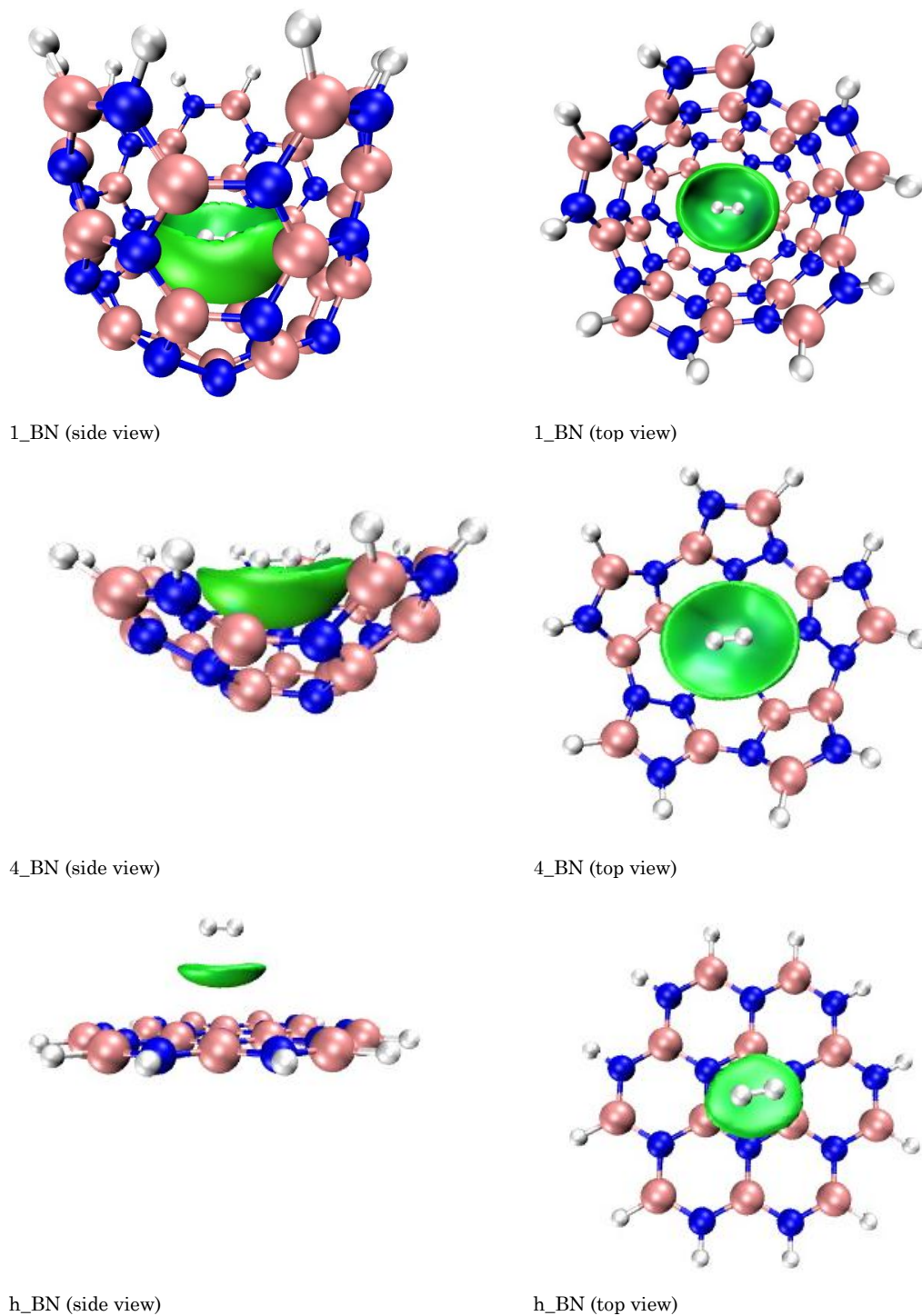


**Fig. 3** – The isosurfaces (green color) of  $\delta^{\text{inter}}$  (isovalue = 0.04) for 1\_BN, 4\_BN, and h\_BN. Atomic color code: blue – nitrogen, pale red – boron, white – hydrogen

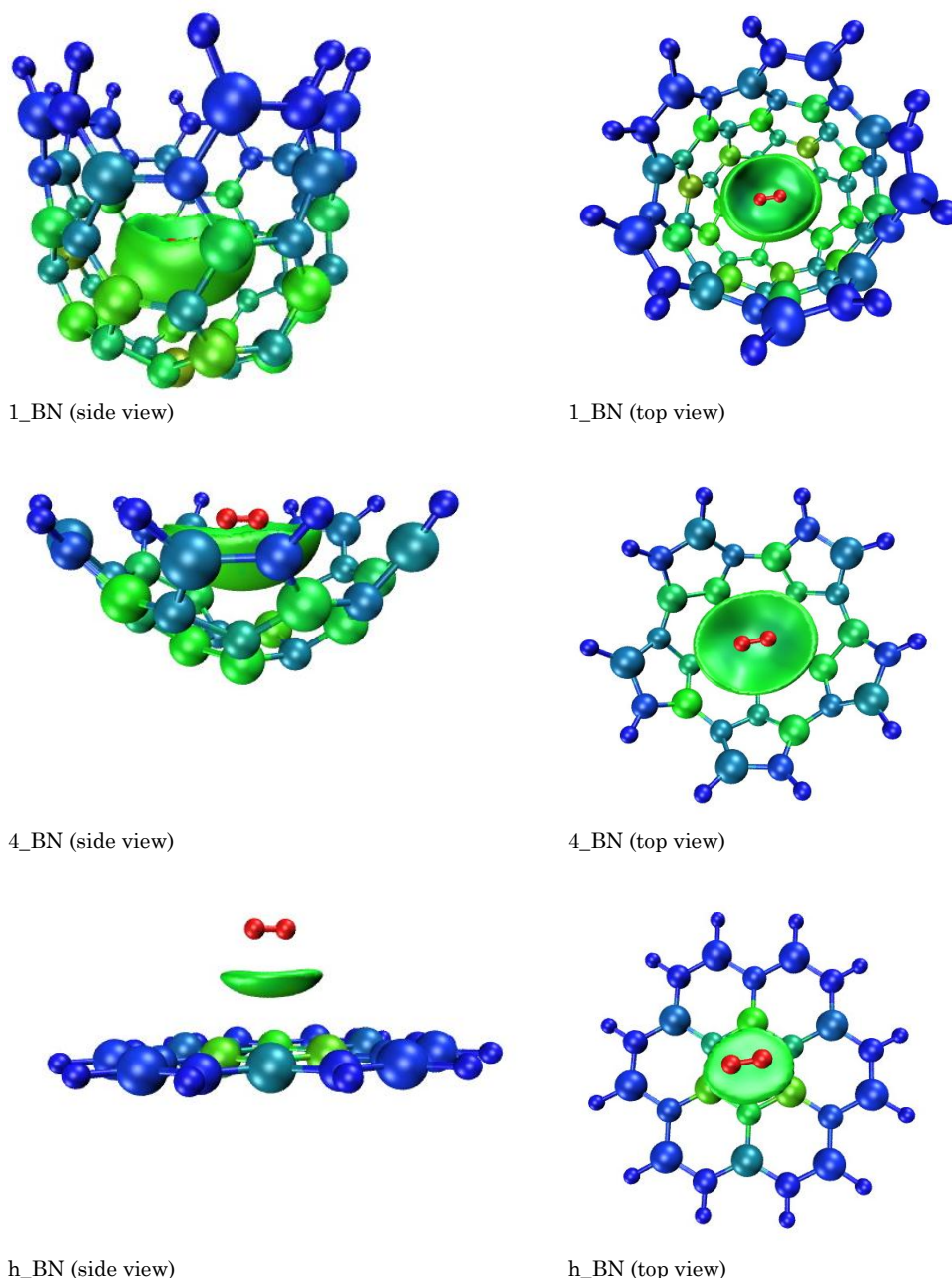


**Fig. 4** – Inputs of the atoms in intermolecular interactions for 1\_BN, 4\_BN, and h\_BN. Blue denotes weak, green – intermediate, red – strong interactions. Small balls are hydrogen, middle balls are nitrogen, large balls are boron. For the isosurfaces, isovalue was set to 0.04

For isosurfaces obtained *via* the IGM analysis, the default color scheme is Blue-Green-Red. The more blue the isosurface, the stronger the attractive interactions; the more red the isosurface, the larger the steric effects. Green color of the isosurface shows that the corresponding interactions are weak and may be regarded as non-covalent interactions.

Fig. 3 shows that the only type of H<sub>2</sub>/adsorbents interactions is a weak Van der Waals interaction. The isosurfaces represent the weak interaction region between hydrogen and all studied systems very clearly. The shape of the isosurface reflects the shape of the respective adsorbent. For the deeper models, the isosurfaces also have the bowl-like shapes, while for the flat h\_BN we can observe the nearly flat isosurface.

The volume of the isosurfaces qualitatively repeats the interaction strength. The graphical data are in accordance with the calculated  $E_a$  values (Table 1). Thus, we can conclude that there is a direct dependence of the  $E_a$  on the pore depths or, in other words, on the number of atoms surrounding the hydrogen molecule. However, we can see that despite the differences in bowl depths for 1\_BN and 2\_BN (the latter is not shown in Fig. 3), the volumes of the isosurface for them are almost the same (as well as the  $E_a$  values for these adsorbents). We can, therefore, conclude that the adsorption energy between hydrogen and the studied adsorbent gets closer to saturation. Indeed,  $E_a$  for the h\_BN model is  $-3.55$  kJ/mol. The  $E_a$  value increases approximately five times on going from h\_BN to the 2\_BN model

(− 18.73 kJ/mol), and there is only a small increment in  $E_a$  (19.77 kJ/mol) when we study adsorption on 1\_BN model. To show unambiguously the relative unimportance of the boron and nitrogen peripheral atoms, we also employ the IGM approach.

As we mentioned earlier, using the IGM analysis, we can obtain  $\delta g$  indices, i.e. the relative importance of various atoms for interfragment interactions can be easily calculated. We then add atom indices  $\delta g$  on molecular structures, and, thereby, show the atoms of great importance for non-covalent interactions. The  $\delta g^{\text{inter}}$  isosurfaces are also shown (Fig. 4). The used color scheme is also Blue-Green-Red. However, in the present case, the more red the color of the atom, the larger the atom indices  $\delta g$ , and, therefore, their contribution into interactions. The green atoms can be regarded as of intermediate importance for interfragment interactions. Contributions of the blue atoms to such interactions can be neglected. We, firstly, should note that the peripheral H atoms of 1\_BN make very minor input into the non-covalent interactions. Moreover, the same holds true for all studied adsorbents, i.e. the saturation with H does not lead to the changes of the important studied parameter ( $E_a$ ).

Besides, for 1\_BN, the two upper rows of atoms show minor input into interactions. For 4\_BN, only the peripheral H atoms give zero donations, whereas B and N atoms (light-blue color) add a something more pronounced input into the H<sub>2</sub>/4\_BN interactions. For h\_BN, similar to the case of 1\_BN, the two peripheral rows give approximately zero input into interactions. This suggests, firstly, that the depth of the pore has limited effect on the adsorbed H<sub>2</sub> molecule. We can see that the further increase of the pore depths does not give significant increase in non-covalent interactions and, therefore,  $E_a$  values. Secondly, the flattening of the adsorbent makes the distances between the H<sub>2</sub> molecule and the peripheral atoms longer. Such a situation, therefore, switches off the atoms from the interactions and diminishes the  $E_a$  value. It indicates the principal importance of the pores in the H<sub>2</sub>/adsorbent interactions. This situation can be clearly observed in Fig. 4 (top views of all studied models). In fact, only six

atoms participate in the the H<sub>2</sub>/h\_BN interactions. For the H<sub>2</sub>/4\_BN, we note the double increase in the quantity of participating atoms. In the case of the deepest studied model, 1\_BN, the quantity increases much more. However, as we mentioned above, the further increase of the pore depth does not lead to the  $E_a$  enhancement.

We believe that the results derived in this theoretical work are valuable for the understanding of the physical mechanisms of hydrogen storage using BN pores to design new materials for hydrogen storage.

#### 4. CONCLUSIONS

In summary, five single-walled boron nitride pores are simulated to study the effect of depths on interactions between them and hydrogen molecules. The obtained results have been compared with those on planar h\_BN. It has been established that the deepest pores, 1\_BN and 2\_BN, can store H<sub>2</sub> with  $E_a$  of − 19.77 and − 18.73 kJ/mol, respectively. These energies lie within the optimal range of H<sub>2</sub> adsorption energy for hydrogen storage. The fundamental physical mechanism underlying the non-covalent interactions between the pores and hydrogen has been revealed by using IGM analysis. We visualize the domains corresponding to the non-covalent interactions and show the atoms participating in the interactions more. We have shown that the further increase in the pore depths does not lead to the increase of  $E_a$ . The present analysis may be used for realization of a novel hydrogen storage material for energy application.

#### 5. ACKNOWLEDGEMENTS

This work was partially supported by the base part of the Government Assignment for Scientific Research from the Ministry of Science and Higher Education of Russia (project code: 13.7232.2017/8.9), Mikhail Lomonosov grant of the Government Assignment for Scientific Research from the Ministry of Science and Higher Education of Russia (project code: 4.13413.2019/13.2), and IRNITU grant for scientific groups (No. 03-FPK-19).

#### REFERENCES

1. K. Alanne, S. Cao, *Renew. Sust. Energ. Rev.* **71**, 697 (2017).
2. N.A.A. Rusman, M. Dahari, *Int. J. Hydrogen Energ.* **41** No 28, 12108 (2016).
3. F. Bonaccorso, L. Colombo, G. Yu, M. Stoller, V. Tozzini, A.C. Ferrari, R.S. Ruoff, V. Pellegrini, *Science* **347**, 1246501 (2015).
4. A. Lale, S. Bernard, U. Demirci, *ChemPlusChem* **83** No 10, 893 (2018).
5. G. Lian, X. Zhang, S. Zhang, D. Liu, D. Cui, Q. Wang, *Energ. Env. Sci.* **5**, 7072 (2012).
6. J. Li, J. Lin, X. Su, X. Zhang, Y. Xue, J. Mi, Z. Mo, Y. Fan, L. Hu, X. Yang, J. Zhang, F. Meng, S. Yuan, C. Tang, *Nanotechnology* **24**, 155603 (2013).
7. I.K. Petrushenko, K.B. Petrushenko, *Comput. Theor. Chem.* **1140**, 80 (2018).
8. Q. Weng, X. Wang, C. Zhi, Y. Bando, D. Golberg, *ACS Nano* **7**, 1558 (2013).
9. S. Marchesini, X. Wang, C. Petit, *Front. Chem.* **7**, 160 (2019).
10. G.C. Vougioukalakis, M.M. Roubelakis, M. Orfanopoulos, *Chem. Soc. Rev.* **39**, 817 (2010).
11. F. Neese, *WIREs Comput Mol Sci* **8**, e1327 (2018).
12. S. Grimme, J. Antony, S. Ehrlich, H. Krieg, *J. Chem. Phys.* **132**, 154104 (2010).
13. M.B. Brands, J. Nitsch, C.F. Guerra, *Inorg. Chem.* **57**, 2603 (2018).
14. Y. Okamoto, Y. Miyamoto, *J. Phys. Chem. B* **105**, 3470 (2001).
15. G. Mpoumpakis, G.E. Froudakis, *Catal. Today* **120**, 341 (2007).
16. I.K. Petrushenko, K.B. Petrushenko, *Int. J. Hydrogen. Energ.* **43** No 2, 801 (2018).
17. Q. Sun, P. Jena, Q. Wang, M. Marquez, *J. Am. Chem. Soc.* **128**, 9741 (2006).
18. X. Wu, Y. Gao, X.C. Zeng, *J. Phys. Chem. C* **112**, 8458 (2008).
19. Y. Gao, X. Wu, X.C. Zeng, *J. Mater. Chem. A* **2**, 5910 (2014).
20. Y. Zhou, W. Chu, F. Jing, J. Zheng, W. Sun, Y. Xue, *Appl. Surf. Sci.* **410**, 166 (2017).
21. F.J. Isidro-Ortega, J.H. Pacheco-Sánchez, L.A. Desales-Guzmán, *Int. J. Hydrogen. Energ.* **42**, 30704 (2017).
22. G. Chen, Q. Peng, H. Mizuseki, Y. Kawazoe, *Comput. Mater.*

- Sci.* **49**, S378 (2010).  
23. E.R. Johnson, S. Keinan, P. Mori-Sánchez, J. Contreras-García, A.J. Cohen, W. Yang, *J. Am. Chem. Soc.* **132**, 6498 (2010).  
24. C. Lefebvre, G. Rubez, H. Khartabil, J.-C. Boisson, J. Contreras-García, E. Hénon, *Phys. Chem. Chem. Phys.* **19**, 17928 (2017).

## Пори одношарового нітриду бору як середовище для зберігання водню: DFT і IGM методи

І.К. Петрушенко

*Іркутський національний науково-технічний університет, вул. Лермонтова, 83, Иркутськ 664074, Росія*

Пошук нових середовищ для зберігання водню є важливим для переходу на «зелену» водневу енергетику. У даній роботі ми вивчаємо фізадсорбцію водню на порах одношарового нітриду бору (BN) за допомогою розрахунків DFT-D3. У роботі були задіяні різноманітні структури, від плоскої до порожнистих моделей. Встановлено, що моделі глибоких пор адсорбують молекули  $H_2$  значно сильніше (енергія адсорбції  $E_a$  складає від  $-11.41$  до  $-19.77$  кДж/моль), ніж плоска структура  $h\_BN$  ( $-3.55$  кДж/моль) і злегка зігнута структура  $5\_BN$  ( $6.77$  кДж/моль). Для візуалізації взаємодіючих областей між воднем і серією адсорбентів використовувався додатковий незалежний градієнтний аналіз (IGM). Також ми чітко виявляємо атоми адсорбентів та молекулу адсорбату, що беруть участь у взаємодії. Ми показуємо, що периферійні атоми адсорбентів дають майже незначний внесок у загальну нековалентну взаємодію. Наведені результати повинні розширити розуміння фундаментальної основи зберігання водню з використанням моделей пор нітриду бору.

**Ключові слова:**  $h\_BN$ , Нітрид бору, Водень, DFT, Адсорбція, Пори.